Short Wavelength Seeding through Compression for Free Electron Lasers

Ji Qiang

Lawrence Berkeley National Laboratory,

Berkeley, CA 94720

In this paper, we propose a seeding scheme that compresses an initial laser modulation in the longitudinal phase space of an electron beam by using two opposite sign bunch compressors and two opposite sign energy chirpers. This scheme could potentially reduce the initial modulation wavelength by a factor of C and increase the energy modulation amplitude by a factor of C, where C is the compression factor of the first bunch compressor. Using two lasers as energy chirpers, such a modulation compression scheme can generate kilo-Amper short wavelength current modulation with significant bunching factor from an initial a few tens Amper current. This compression scheme can also be used to generate a prebunched single atto-second short wavelength current modulation and prebunched two color, two atto-second modulations.

The tunable short wavelength free electron lasers (FELs) provide great opportunities for scientific discoveries in biology, chemistry, material science and physics, and form a basis for fourth generation light source. Currently, there are two main approaches used in FEL to generate such short wavelength radiation: one is based on the self-amplified spontaneous emission (SASE) [1, 2], the other is based on the high-gain harmonic generation (HGHG) scheme [3, 4]. The SASE FEL starts from the shot noise radiation of the electron beam. This limits the temporal coherence of radiation output and also results in a relatively large shot-to-shot output fluctuation. In contrast, the HGHG scheme uses laser as an initial signal to modulate the electron beam. The FEL works as a nonlinear amplifier of the initial signal that can generate coherent radiation not only at the fundamental harmonic of the seed laser but also at the higher harmonics. This also gives the FEL radiation from the HGHG scheme a good longitudinal coherence, high stability and shorter saturation length compared with the SASE approach.

The standard single stage HGHG scheme consists of a modulator that converts the laser field oscillation into the electron beam energy modulation through laser-electron resonant interaction

inside an undulator, a dispersive element that converts the electron beam energy modulation into current modulation, and an FEL radiator that produces coherent radiation using a harmonic of electron beam current modulation. The efficiency of this up-frequency conversion is limited by the amplitude of the harmonic component inside the electron beam current modulation that decreases exponentially with the increase of the harmonic number. This limits the harmonic number usually to a small number. To overcome this problem and to reach shorter wavelength radiation, multi-stage HGHG scheme was proposed with significant design and operation complication [5].

Several methods were proposed to improve the up-frequency conversion efficiency of the single stage HGHG with some modest success [6, 7]. Recently, a new approach based on beam echo effect that can significantly improve the up-frequency conversion efficiency was proposed for generation of short wavelength radiation [8]. In that scheme, the energy modulated beam is sent into a dispersive element with stronger compression factor than the normal HGHG dispersive element. This over compressed beam is then sent into another laser-beam modulator to generate fine structure in longitudinal phase space. Such a beam is then sent into another normal dispersive element with small R_{56} to generate high harmonic current modulation. One important advantage of this echo enabled harmonic generation (EEHG) scheme over the standard HGHG is that the bunching factor of the high harmonic decreases only as cubic root of the harmonic number. This enables the EEHG scheme to generate high harmonic current modulation with a reasonable bunching factor.

Both the HGHG and the EEHG require the use of significant amount of laser power to seed the electron beam. In this paper, we propose a new scheme for generating short wavelength radiation by modulation compression. Through modulation compression, the initial energy modulation amplitude can be amplified by a factor of compression factor while the modulation wavelength is reduced by a factor of compression factor. This significantly reduces the laser power needed for the generation of short wavelength radiation. Meanwhile, since the modulation wavelength has already been reduced by the compression factor, a fundamental mode of such modulation can be used directly to produce short wavelength current modulation. This results in a large bunching factor for such a short wavelength modulation. Furthermore, using two lasers as energy chirpers, such a scheme can be used to generate kilo-Amper short wavelength current modulation from an initial a few tens Amper current beam. By using a few cycle laser pulse as the second energy chirper, this scheme can generate a single atto-second and two color, two atto-second prebunched short wavelength pulses.

A schematic plot of the accelerator beam line element for the proposed scheme is shown in Figure 1. It consists of a laser modulator, an energy chirper A, a bunch compressor A, another

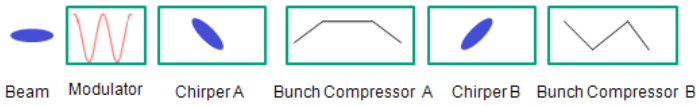

FIG. 1: A schematic plot of the accelerator lattice for modulation compression.

energy chirper B, and another bunch compressor B. In this scheme, an initial laser modulated electron beam is transported through an energy chirper to obtain a negative energy chirp across the beam bunch length. This chirped beam is sent into a standard bunch compressor for bunch compressing. After the bunch compressor, the beam is transported through another energy chirper with opposite sign of energy-bunch length correlation compared with that of the first energy chirper. This chirper undoes the global negative energy chirp across the beam and generates a local positive energy chirp with an amplified energy modulation amplitude. After the second energy chirper, the beam is transported through the second bunch compressor that has opposite sign of R_{56} compared with the first bunch compressor. This bunch compressor further compresses the positive chirped beam and results in a compressed energy modulation with increased modulation amplitude and reduced modulation wavelength. Some similar schemes were proposed by Biedron et al. and Shaftan et al. for tuning HGHG radiation wavelength and by Shintake [9–11]. A key difference between the scheme proposed in this paper and the previous schemes is the usage of the second opposite sign bunch compressor. Without such a bunch compressor, the initial modulation of the beam will not be further compressed while the original modulation structure inside the locally over compressed beam will not contribute to significant current modulation.

In the following, we will derive the longitudinal phase space distribution of beam transporting through above ideal accelerator lattice using a one-dimensional model. The beam is assumed to be longitudinal frozen in most part of the lattice except that in the bunch compressors. The initial longitudinal phase space distribution function before the laser modulator is given as:

$$f_0(z_0, \delta_0) \;=\; F(z_0, \delta_0/\sigma) \tag{1}$$

where z_0 is the longitudinal bunch length, $\delta_0 = \Delta E_0/E_0$ is the relative energy deviation, σ is a constant related to the initial energy spread. After the laser modulator, the energy deviation becomes, $\delta_1 = \delta_0 + A\sin(kz_0)$, where $A = V_1/E_1$ is the initial laser modulation amplitude, $\delta_1 = \Delta E_1/E_1$, $E_1 = E_0$, and k is the modulation wave number. The distribution function after the modulator becomes

$$f_1(z_1, \delta_1) \;=\; F(z_1, \frac{\delta_1 - A\sin(kz_1)}{\sigma}) \tag{2}$$

Now, the beam is transported through the chirper A that will introduce an energy-bunch length correlation, $\delta_2 = D^a\delta_1 + h^a z_1$, where $h^a = d\delta_2/dz_2$ is the energy chirp across the bunch length of the beam, $\delta_2 = \Delta E_2/E_2$, and $D^a = E_1/E_2$ denotes the ratio of total beam energy before and after the chirper A. The longitudinal phase space distribution after this chirper becomes

$$f_2(z_2,\delta_2) \;=\; \frac{1}{D^a}F(z_2, \frac{\delta_2 - h^a z_2 - D^a A\sin(kz_2)}{D^a\sigma}) \tag{3}$$

Next, the beam passes through the bunch compressor A. The longitudinal bunch length becomes, $z_3 = z_2 + R^a_{56}\delta_2$, where R^a_{56} is the momentum compaction factor of the bunch compressor A. After the bunch compressor, the phase space distribution becomes

$$f_3(z_3,\delta_3) \;=\; \frac{1}{D^a}F(z_3 - R^a_{56}\delta_3, \frac{\delta_3 - h^a C z_3 - CD^a A\sin(k(z_3 - R^a_{56}\delta_3))}{CD^a\sigma}) \tag{4}$$

where $C = 1/(1 + R^a_{56}h)$ is the bunch compression factor of the first bunch compressor A. Then the beam is transported through the chirper B that will introduce another energy-bunch length correlation, $\delta_4 = D^b\delta_3 + h^b z_3$, where h^b is the energy chirp across the bunch length of the beam caused by the second chirper, $D^b = E_3/E_4$ denotes the ratio of total beam energy before and after the chirper B, and $\delta_4 = \Delta E_4/E_4$. The phase space distribution becomes

$$\begin{aligned} f_4(z_4,\delta_4) \;=\; & F(z_4(D^b + h^b R^a_{56})/D^b - R^a_{56}/D^b\delta_4, \\ & \frac{\delta_4 - (h^b + h^a D^b C)z_4 - CD^b D^a A\sin(k(z_4(D^b + R^a_{56}h^b)/D^b - R^a_{56}/D^b\delta_4))}{CD^b D^a\sigma}) \end{aligned} \tag{5}$$

If the second chirper is set up so that $h^b = -h^a D^b C$, then the distribution function can be written as

$$f_4(z_4,\delta_4) \;=\; \frac{1}{D^a D^b}F(Cz_4 - R^a_{56}/D^b\delta_4, \frac{\delta_4 - CD^b D^a A\sin(kCz_4 - kR^a_{56}/D^b\delta_4)}{CD^b D^a\sigma}) \tag{6}$$

Finally the beam is transported through the second bunch compressor B. The longitudinal bunch length of the beam becomes, $z_5 = z_4 + R^b_{56}\delta_4$, where R^b_{56} is the momentum compaction factor of the bunch compressor B. The final longitudinal phase space distribution becomes

$$f_5(z_5,\delta_5) \;=\; \frac{1}{D^a D^b}F(Cz_5 - (R^b_{56} + R^a_{56}/D^b)\delta_5, \frac{\delta_5 - CD^b D^a A\sin(kCz_5 - (kCR^b_{56} + kR^a_{56}/D^b)\delta_5)}{CD^b D^a\sigma}) \tag{7}$$

If the second bunch compressor is set up so that $R^b_{56} = -R^a_{56}/(D^b C)$, then the final longitudinal distribution function can be written as

$$f_5(z_5,\delta_5) \;=\; \frac{1}{D^a D^b}F(Cz_5, \frac{\delta_5 - CD^b D^a A\sin(kCz_5)}{CD^b D^a\sigma}) \tag{8}$$

Comparing this distribution function f_5 with f_1 after the laser modulator, we see that the longitudinal modulation wavelength is reduced by a factor of C and the relative amplitude of modulation

is increased by a factor of D^bD^aC. Writing the final energy modulation amplitude in absolute unit of energy, this results in a final energy modulation amplitude CV_1 (eV), where V_1 is the initial absolute energy modulation amplitude due to the laser beam interaction inside the modulator.

As a numerical illustration, we assume $D^a = D^b = 1$ (i.e. no acceleration through the proposed accelerator lattice), initial uniform current distribution and Gaussian energy distribution with a relative energy spread $\sigma = 0.5 \times 10^{-4}$, initial relative modulation amplitude $A = 2 \times 10^{-4}$, initial laser modulation wavelength 1 um, the first chirp $h^a = -19$ (m^{-1}), the first bunch compressor $R^a_{56} = 5$ cm, the second chirp $h^b = 380$ (m^{-1}), and the second bunch compressor $R^b_{56} = -2.5$ mm. This will result in a compression factor 20 from the first bunch compressor. Figure 2 shows the two-period longitudinal phase space of the beam after the initial modulation, after the first chirper A, after the first bunch compressor A, after the second chirper B, and after the second bunch compressor B. It is seen that the initial chirped modulation is significantly over compressed after the first bunch compressor as shown in the plot (c) of the figure. There is little current modulation in this situation. After the second chirper, the beam is counter-clockwise rotated to remove the global negative chirp. The two-period modulation structure is barely seen in this local positively chirped beam while the amplitude of the modulation increases by a factor of 20. After the second bunch compressor with negative R_{56}, the beam is further compressed longitudinally. This restores the initial energy modulation structure as shown in the last plot of the Figure 2. The final modulation wavelength is reduced from the initial 1 um down to 0.05 um while the modulation amplitude increases from 3.5×10^{-4} to 7.0×10^{-4} as expected.

The above compressed energy modulation will not generate current modulation directly. However, by tuning the R^b_{56} of the second bunch compressor, a strong current modulation with reduced wavelength will appear. This is similar to the standard process of high harmonic generation [4]. Assume an initial uniform current distribution with a Gaussian energy distribution, the longitudinal phase space distribution after the modulation compression can be written as:

$$f_5(z_5, \delta_5) \;=\; \exp(-\frac{1}{2}(\frac{\delta_5 - CD^bD^aA\sin(kCz_5 - (kCR^b_{56} + kR^a_{56}/D^b)\delta_5)}{CD^bD^a\sigma})^2) \tag{9}$$

Now, if the R^b_{56} of the second bunch compressor B is not exactly set as $-R^a_{56}/(D^bC)$ but with a small deviation, i.e. $R^b_{56} = -R^a_{56}/(D^bC) + \Delta r^b$, then the distribution function after the bunch compressor B will be

$$f(z, \delta) \;=\; \exp(-\frac{1}{2}(\frac{\delta - CD^bD^aA\sin(kCz - kC\Delta r^b\delta)}{CD^bD^a\sigma})^2) \tag{10}$$

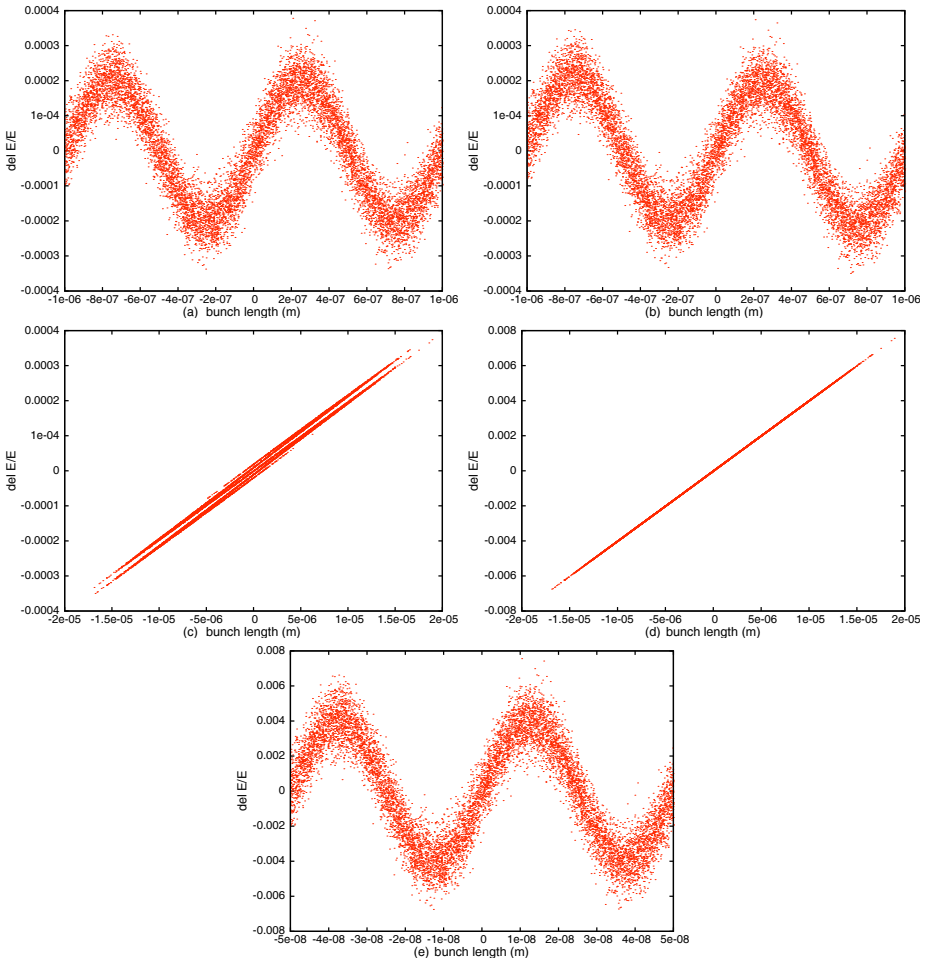

FIG. 2: Two-period longitudinal phase space evolution after initial modulation (a), after the first chirper (b), after the first chicane bunch compressor (c), after the second chirper (d), and after the second bunch compressor (e).

The current distribution $I(z)$ can be found from integration of the above distribution over δ:

$$I(z) \;=\; \int_{-\infty}^{\infty} d\delta \;\exp(-\frac{1}{2}(\frac{\delta - CD^bD^aA\sin(kCz - kC\Delta r^b\delta)}{CD^bD^a\sigma})^2) \tag{11}$$

This integral has the same form as that in the standard high harmonic generation scheme[4]. It is a periodic function of z and can be represented as a Fourier series yielding [12]:

$$I(z) \;=\; I_0(1 + 2\sum_{n=1}^{\infty} b_n \cos(nCkz)) \tag{12}$$

where the coefficient b_n (i.e. bunching factor of harmonic n) is given as

$$b_n \;=\; J_n(nC^2k\Delta r^bAD^bD^a)\exp(-\frac{1}{2}n^2(C^2k\Delta r^bD^bD^a\sigma)^2) \tag{13}$$

where the J_n is the Bessel function of order n. From above equation, it is seen that the bunching factor has a strong dependence on the harmonic number. Since the initial modulation wavelength

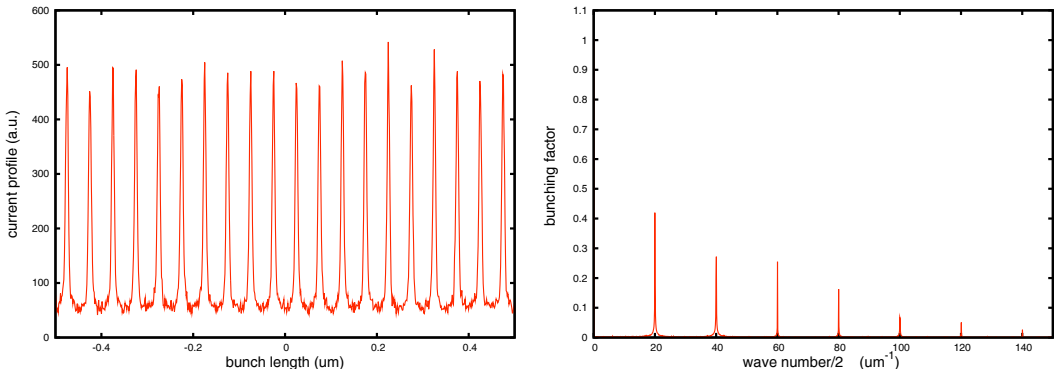

FIG. 3: Current profile (left) and bunching factor (right) of the beam after the second bunch compressor with detuned R_{56}.

has already been compressed by a factor of C, it might be sufficient to use fundamental harmonic ($n = 1$) for short wavelength FEL radiation. Following the concept of high harmonic generation, we can also optimize the design for higher harmonic number. This might result in an even shorter wavelength radiation with a wavelength $\lambda/(nC)$, where λ is the seed laser wavelength. From Eq. 13, we can see that the bunching factor also depends strongly on the products of compression factor of the first bunch compressor and the Δr^b of the second bunch compressor. Without using the second bunch compressor, i.e. $R^b_{56} = 0$ or $\Delta r^b = R^a_{56}/(D^b C)$, with a compression factor of 20 from the first bunch compressor in above numerical example, this will result in a very large exponential decreasing factor (10^{-49348}) in the bunching factor of the initial 1 um wavelength modulation even for the fundamental harmonic. In order to maximize the bunching factor for high harmonic generation, the R^b_{56} of the second bunch compressor needs to be carefully chosen so that Δr^b is sufficiently small to minimize the exponentially decreasing factor in Eq. 13 while maximizing the Bessel function contribution. As an illustration, using the preceding numerical example, we set the R^b_{56} of the second bunch compressor 0.1% off the matched value. Figure 3 shows the current distribution and the bunching factor of the beam after the second bunch compressor B with small offset of the R^b_{56}. Very strong current modulation at the wavelength of 0.05 um is observed in the left plot of the Figure 3. From the right plot of the Figure 3, we see that there also exists significant extent of bunching factor even for 4th order harmonic that corresponds to a wavelength of 12.5 nm.

Significant amount of energy chirp is needed in the proposed scheme as shown in above example. When a beam pass through a section RF linac, the energy chirp factor h across the beam is given

by

$$h \;=\; \frac{eV}{E} k_{rf} \sin(\phi) \tag{14}$$

where V is the maximum voltage gain through the chirper, E is the final energy of the beam, k_{rf} is the wave number of the RF wave inside the cavity, ϕ is the synchronous phase between the electron beam and the RF wave. At a fixed energy (i.e. $\phi = \pi/2$), in order to achieve a large energy chirp, a shorter wavelength RF cavity will be better. For a beam passing through an RF linac of 1.3 GHz, it requires 174.5 MeV to generate an energy chirp of 19 (m^{-1}), and 3.49 GeV to unchirp the beam after a factor of 20 compression. Such a energy chirp requires a large amount of conventional RF power and a long distance of linac accelerating structure. In this regard, a high power laser might be more suitable as a chirper. In the following example, we propose using a 10 um laser as chirper A and chirper B to compress an initial 200 nm modulation down to 2 nm as an illustration of above compression scheme. Here, the laser chirper will provide a local periodic energy modulation across the beam by resonant interaction between the laser field and the electron beam inside a short undulator. (This is the same mechanism as the modulator.) Since the chirper laser wavelength is much longer than the seeding laser wavelength, those long wavelength energy modulation provides a local periodic chirping for the initial modulated electron beam. In this example, we assume that a uniform 20 pC, 2.5 GeV electron beam with 100 um bunch length and 10^{-5} relative slice energy spread is initially modulated by a 200 nm seed laser. The relative energy modulation amplitude is set as 2×10^{-5}. The initial 10^{-5} slice energy spread is feasible given the low current of the beam (60 A). Such a low current beam can be produced directly from a photoinjector and transports through accelerating linac without resorting to bunch compressors to increase the peak current, which also increases the slice energy spread. The slice energy spread out of the photoinjector can be on the order of a few keV [13]. This gives the final relative slice energy spread at 2.5 Gev below 10^{-5}. Figure 4 shows the relative energy modulation for the laser chirper A and the laser chirper B. The energy modulation in the first laser chirper is about 0.25 MeV at 2.5 GeV beam energy. The relative energy modulation in the laser chirper B is 1%, which corresponds to 25 MeV energy modulation. The energy chirp at the zero field crossing from the first laser chirper is about -62.8 (m^{-1}). The compression factor of the first bunch compressor is set as 100 so that the initial 200 nm modulation can be compressed down to 2 nm. For such a compression factor the R_{56} of the first bunch compressor is 1.6 cm. The R_{56} of the bunch compressor B is -0.16 mm. Figure 5 shows the peak current distribution after the bunch compressor B in this example. It is seen that after the second bunch compressor, there are a sequence of local current peaks with more than 7

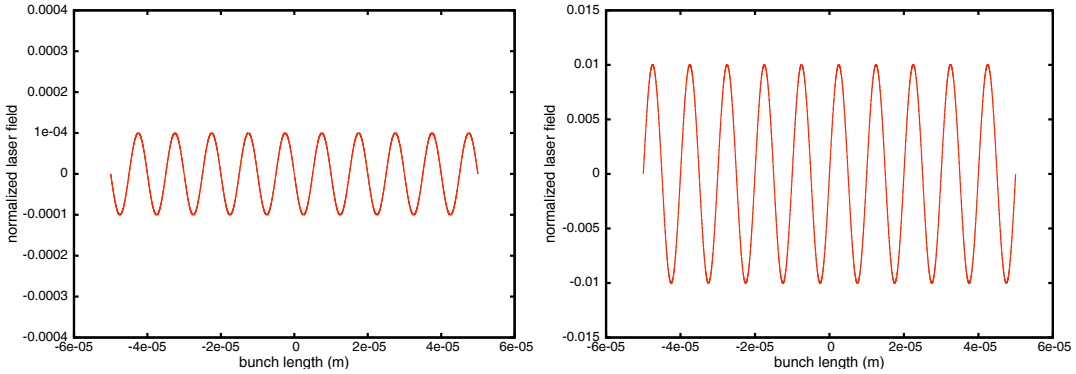

FIG. 4: Relative energy modulation from the laser chirper A (left) and the laser chirper B (right).

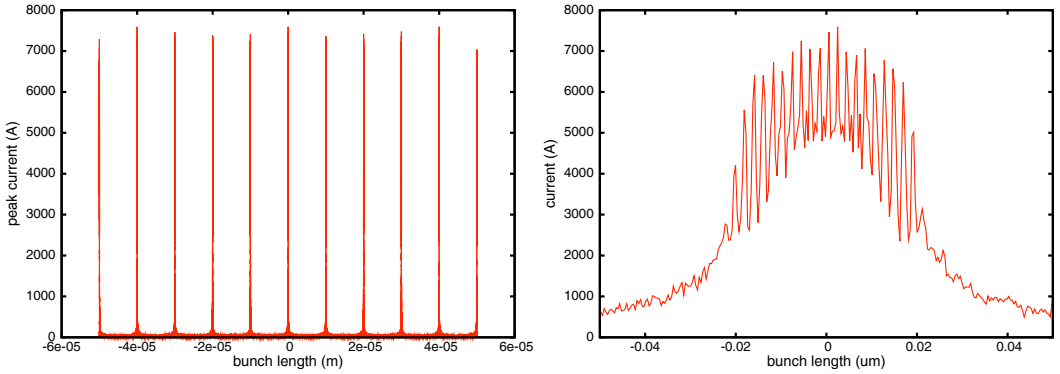

FIG. 5: Total peak current distribution and a room-in current distribution around 0 um (right) location after the bunch compressor B.

kilo-Amper current. Those periodic high current peaks are separated by 10 um controlled by the first chirper laser wavelength. Inside each local current peak, as shown in the right plot of the Figure 5, there are a number of current peaks (around 20) with a separation of 2 nm resulting from the compression of the initial 200 nm seeding laser modulation. Those micro-current peaks result in a large bunching factor for the 2 nm modulation. Figure 6 shows the longitudinal phase space around the center of the beam after the bunch compressor B. The initial 200 nm modulation is compressed down to 2 nm modulation with a local energy modulation amplitude around 0.4%. Those short wavelength modulations contribute to the local high peak current modulation shown in Figure 5. In above example, a sequence of high current peaks are produced with a width of about 50 nm (170 as) from an initial low current beam. Such a prebunched short wavelength modulated beam can be sent to a radiator to generate a sequence of atto-second short wavelength radiation. It might also be sent to a sequence of short periods (around 20) undulators with appropriate phase shifter to generate high power seeded FEL radiation.

In recent years, there are also growing interests in generating single atto-second x-ray radiation

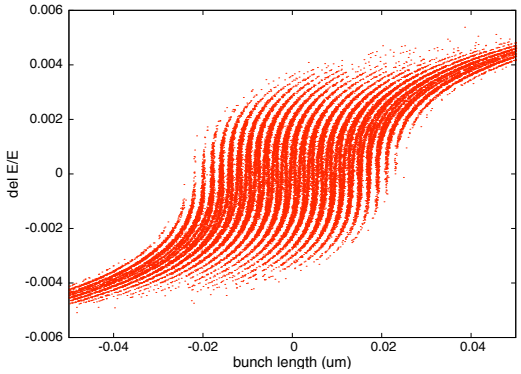

FIG. 6: Longitudinal phase space distribution around 0 um after the bunch compressor B.

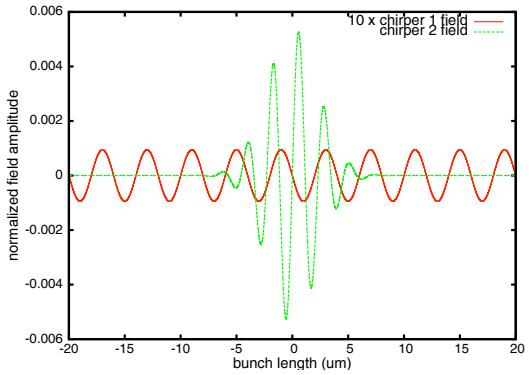

FIG. 7: Relative energy modulation from the laser chirper A and the laser chirper B.

using FELs [14–20]. In the following, we propose using two laser chirpers with different wavelengths to generate a single atto-second current peak with short wavelength modulation. We assumed the same electron beam parameters as the preceding example. A 200 nm UV seed laser is used to generate initial 2×10^{-5} relative energy modulation. Figure 7 shows the energy modulation/local chirping from the two laser chirpers. The first laser has 4 um wavelength providing about 10^{-4} initial relative energy modulation. This laser will generate a sequence of local chirp of the initially modulated beam with 4 um separation. The second laser has a few cycle pulse length with a wavelength of 2.3 um, which is chosen to mismatch the locations of the first laser chirping except for the center of the beam. Only those modulated electrons located around the center of the beam will be correctly chirped and unchirped. The electrons at other locations that are not correctly chirped and unchirped will not be compressed correctly after the second bunch compressor. The R_{56} of the first bunch compressor is 6.7 mm with a compression factor of 100. The R_{56} of the second bunch compressor is -0.067 mm. Figure 8 shows current distribution of the electron beam after the second bunch compressor in this example. Here only a single high current peak (around 6 kA) is observed in the beam with more than an order of magnitude contrast compared with background

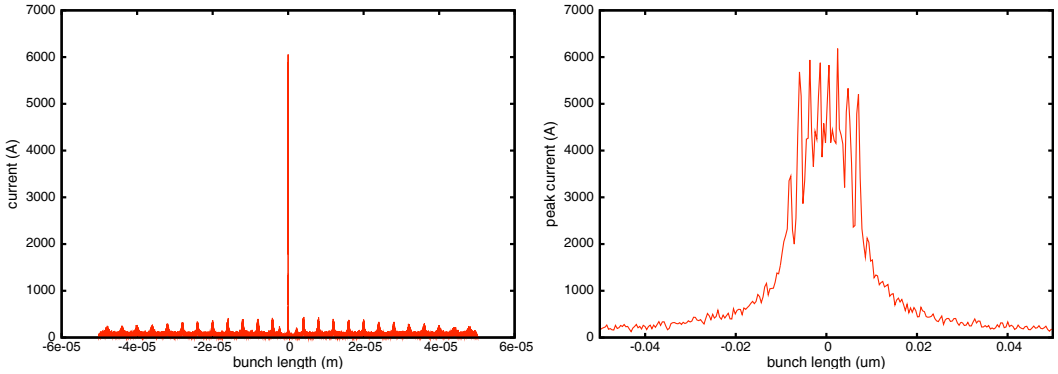

FIG. 8: Total current distribution (left) and room-in current distribution after the second bunch compressor.

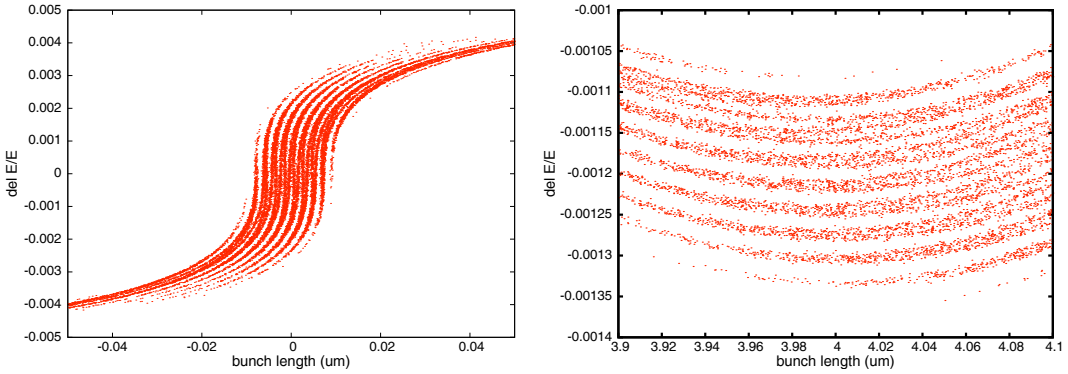

FIG. 9: Longitudinal phase space distribution around the center of the beam (left) and 4 um away from the center (right) after the bunch compressor B.

current. The room-in plot of the local current peak (right plot of the figure) shows that the local current peak has a width of about 20 nm (70 atto-seconds) with prebunched 2 nm wavelength current modulation. Figure 9 shows the longitudinal phase space distribution around the center of the beam and 4 um away from the center after the second bunch compressor. It is seen that those initial 200 nm modulated electrons around the center of the beam are appropriately compressed by a factor of 100 down to 2 nm wavelength modulation while the electrons at a sequence of 4 um away are over compressed. Those over compressed electrons will not contribute to significant amount of local current.

In the preceding example, only a local high current peak around the center of the beam is used for generating a single atto-second current modulation for a single atto-second pulse X-ray radiation. In another application, two color, two atto-second pulses are proposed for pump-probe experiment [21]. In the following example, we will extend the above single atto-second pulse scheme to generate two color, two atto-second current modulations. A schematic plot of this scheme is shown in Figure 10. Here, after generating the first atto-second current modulation using two

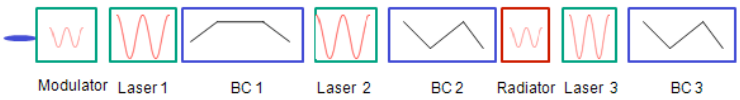

FIG. 10: A schematic plot of the lattice set up for generation of two color, two atto-second pulse prebunched short wavelength current modulation.

laser chirpers based on the modulation compression method in the preceding example, the beam is sent into a short radiator to produce a 2 nm atto-second X-ray radiation. After the beam passes through the radiator, a third a few cycle laser with the same wavelength as the second laser but different amplitude is introduced to unchirp electrons at another location of the beam. After those electrons are unchirped, a third bunch compressor is used to tune the compression factor so that the second atto-second current modulation after the bunch compressor will have a different current modulation wavelength. Since only a few cycle laser is used as the second chirper, outside the pulse length of this laser, at the location of the integer multiple of the first laser chirper wavelength, those locally chirped electrons will be over compressed by the first bunch compressor and the second bunch compressor. Figure 11 shows the longitudinal phase space around the location of 28 um of the beam after the second bunch compressor. After the beam passes through the radiator, those electrons will be subject to local unchirping of the third laser. Figure 12 shows the energy modulation from the first laser, the second laser, and the third laser. The wavelength of the third laser is chosen as the same as the second laser with a different modulation amplitude. The R_{56} of the third bunch compressor is chosen as -0.099 mm, which gives a total compression factor of 67 after the third bunch compressor. Figure 13 shows the current distribution after the third bunch compressor. A high current peak (around 5 kA) is seen around the location of 28 um of the beam. The full width of this current peak is about 30 nm (100 as) with 3 nm modulation wavelength. Such a prebunched beam passes through another radiator to generate a 3 nm atto-second X-ray radiation. This second atto-second X-ray pulse can be used to probe excited electron states inside atoms for the pump-probe experiment.

A number of factors that could affect the performance of the above proposed compression seeding scheme. The modulation structure of the beam after the second bunch compressor depends on the line thickness of the modulation. When the line thickness is greater than the half wavelength, the sinusoidal modulation structure will be lost. Here the wavelength is the final seeding wavelength after compression. Using a one-dimensional model, the longitudinal line thickness after the second

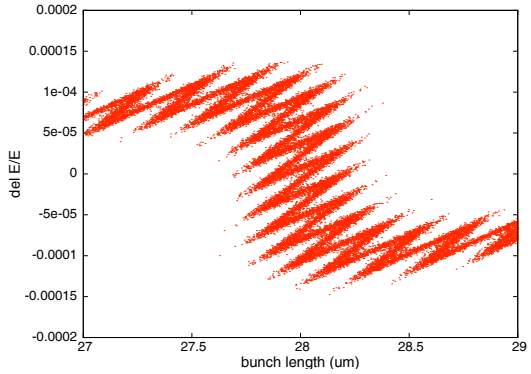

FIG. 11: Local longitudinal phase space around the location of 28 um of the beam after the second bunch compressor.

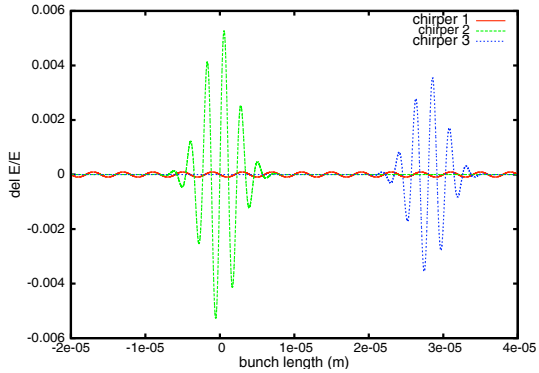

FIG. 12: The energy modulation from the first laser chirper, the second laser chirper and the third laser chirper for generating two color, two atto-second pulses short wavelength modulation.

bunch compressor can be written as:

$$\sigma_{z_5} = \sqrt{\sigma_{z_4}^2 + (R_{56}^b)^2 \sigma_{\delta_4}} \tag{15}$$

where σ_{z_4} is the longitudinal line thickness before the second bunch compressor and σ_{δ_4} is the local energy spread of each modulation period before the second bunch compressor.

The finite energy spread δ inside a beam contributes to longitudinal line thickness after transporting distance L by:

$$\sigma_z = \frac{L}{\gamma^2}\delta \tag{16}$$

where γ is the relativistic energy factor. The finite transverse emittance ϵ of a beam also contributes to longitudinal line thickness after transporting distance L by:

$$\sigma_z = \frac{L}{\gamma^2}\frac{\epsilon}{\beta_l} \tag{17}$$

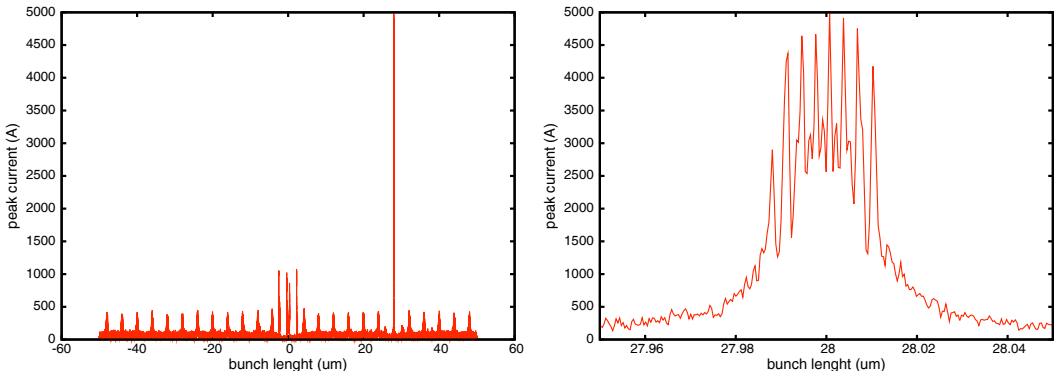

FIG. 13: Total current distribution (left) and room-in current distribution (right) after the third bunch compressor.

where β_l is the average lattice β function. From above two equations, we see that in order to minimize the longitudinal line thickness for a given energy spread and finite emittance, it is preferable to keeping a shorter transport distance at higher energy for the modulated beam.

Collective effects such as wake field, coherent synchrotron radiation and space-charge effects could cause the increase of the energy spread and smear out the modulation structure. The wake field and coherent synchrotron radiation primarily contribute to the correlated energy-bunch length chirp across the beam [22] while the space-charge effects can also cause significant local uncorrelated energy spread through the accelerator. To test the effects from the longitudinal space-charge, we ran a simulation using an updated version of the IMPACT code [23] for a beam with 250 MeV kinetic energy by inserting a drift space between the first bunch compressor A and the chirper B in the layout of the Figure 1. The beam has an initial uniform cylindric distribution in spatial and Gaussian distribution in momentum. The initial transverse beam radius is 1 mm with 1 mm-mrad emittance. The initial uncorrelated energy spread is about 5 keV with a modulation amplitude of 20 keV. The initial modulation wavelength is 1 um and final modulation wavelength after compression is 50 nm. Figure 14 shows the final two-period longitudinal phase space after compression with 0 meter drift space and with 200 meter drift between the first bunch compressor and the second energy chirper. It is seen that the initial energy modulation after the compression is smeared out due to the local energy spread induced by the space-charge effects during the 200 meter drift. This effect could be mitigated by reducing the transport distance between the first bunch compressor and the second bunch compressor and by modulating the beam at higher energy.

The quantum fluctuation of electron incoherent synchrotron radiation inside a bending magnetic can also induce uncorrelated slice energy spread and distort the modulation structure inside the beam. This effect depends on the energy of electron beam, the bending radius of magnet, and

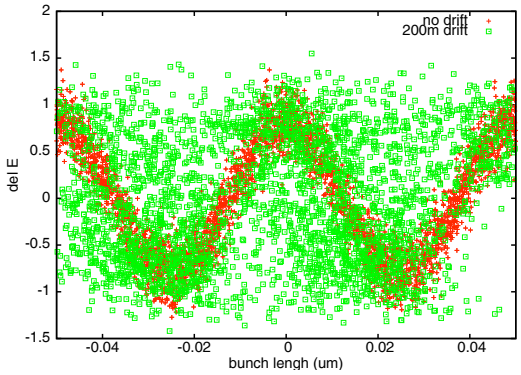

FIG. 14: Two period longitudinal phase space distribution for a cylinder beam without and with drifting 200 meters.

the arc length of the bending magnet. From the previous study [21], it was shown that at an electron beam energy of 2.4 GeV, with $R_{56} = 17.63$ mm of a chicane, this energy spread can be controlled below 3 keV after passing through the chicane. Such an energy spread could be tolerable for generating short wavelength seeding by keeping the R_{56} of the second bunch compressor below 1 mm.

I. SUMMARY AND DISCUSSIONS

In summary, the modulation compression scheme can provide potential advantages for generating tunable short wavelength current modulation for FEL radiation with a large bunching factor. It also provides potential capability to use initial low current beam to generate short wavelength, kilo-Amper current, atto-second prebunched modulation for FEL radiation. Using such a low initial current has advantages of achieving better transverse emittance from the photoinjector, avoiding the use of the magnetic bunch compressor inside the linac, and significantly mitigating the collective effects through the beam delivery system.

A number of factors that could degrade the performance of above modulation compression scheme. From above study, we see that the effects of initial energy spread, transverse emittance, space-charge effects can be significantly reduced by doing the modulation compression at high beam energy. A shorter distance between two bunch compressors also helps reduce those effects. The structure wakefield and coherent synchrotron radiation will affect the long range scale of the density distribution and might not affect the short wavelength modulation. The incoherent synchrotron radiation increases the local energy spread and can be minimized by choosing a smaller R_{56} of the bunch compressor and by using a larger bending radius. Besides those effects, the accelerator

machine nonlinearity needs to be corrected using appropriate beam line element. The machine and laser jitter should also be minimized with feed back system and careful design.

ACKNOWLEDGEMENTS

We would like to thank Drs. J. Corlett, B. Fawley, G. Penn, R. Ryne, C. Toth, M. Venturini, J. Wu, A. Zholents for useful discussions. This research was supported by the Office of Science of the U.S. Department of Energy under Contract No. DE-AC02-05CH11231. This research used resources of the National Energy Research Scientific Computing Center.

REFERENCES

[1] A. Kondratenko and E. Saldin, Part. Accel. 10, 207 (1980).

[2] R. Bonifacio, C. Pellegrini, and L. M. Narducci, Opt. Commun. 50, 373 (1984).

[3] R. Bonifacio, L. D. S. Souza, P. Pierini, and E. T. Scharlemann, Nucl. Instrum. Methods Phys. Res., Sect. A 296, 787 (1990).

[4] L. Yu, Phys. Rev. A 44, 5178 (1991).

[5] J. Wu, L. Yu, Nucl. Instrum. Methods Phys. Res., Sect. A 475, 104 (2001).

[6] E. Allaria and G. De Ninno, Phys. Rev. Lett **99**, 014801 (2007).

[7] Q. Jia, Appl. Phys. Lett **93**, 141102 (2008).

[8] G. Stupakov, Phys. Rev. Lett **102**, 074801 (2009).

[9] S. G. Biedron, S. V. Milton, and H. P. Freund, Nucl. Instrum. Methods Phys. Res., Sect. A **475**, 401 (2001).

[10] T. Shaftan and L. Yu, Phys. Rev. E **71**, 046501 (2005).

[11] T. Shintake,in Proceedings of FEL 2007, Novosibirsk, Russia, p. 378, (2007).

[12] E. L. Saldin, E. A. Schneidmiller, and M. V. Yurkov, Nucl. Instrum. Methods Phys. Res., Sect. A **490**, 1 (2002).

[13] R. Akre et al., Phys. Rev. ST Accel. Beams 11, 030703 (2008).

[14] A. A. Zholents and W. M. Fawley, Phys. Rev. Lett. 92, 224801 (2004).

[15] A. A. Zholents and G. Penn, Phys. Rev. ST Accel. Beams 8, 050704 (2005)

[16] E. L. Saldin, E. A. Schneidmiller, and M. V. Yurkov, Phys. Rev. ST Accel. Beams 9, 050702 (2006)

[17] J. Wu, P. R. Bolton, J. B. Murphy, K. Wang, Optics Express 15, 12749, (2007).

[18] A. A. Zholents and M. S. Zolotorev, New Journal of Physcis 10, 025005 (2008).

[19] Y. Ding, Z. Huang, D. Ratner, P. Bucksbaum, and H. Merdji Phys. Rev. ST Accel. Beams 12, 060703 (2009).

[20] D. Xiang, Z. Huang, and G. Stupakov Phys. Rev. ST Accel. Beams 12, 060701 (2009).

[21] A. A. Zholents and G. Penn, Nucl. Instrum. Methods Phys. Res., Sec A 612, 254 (2010).

[22] E. Kur, G. Penn, J. Qiang, M. Venturini, R. P. Wells, A. Zholents, LBNL-2670E, Sep. 1, 2009.

[23] J. Qiang, R. D. Ryne, M. Venturini, A. A. Zholents, I. V. Pogorelov, Phys. Rev. ST Accel. Beams **12**, 100702, (2009).